

# Cytotoxicity, intracellular localization and exocytosis of citrate capped and PEG functionalized gold nanoparticles in human hepatocyte and kidney cells

Nonhlanhla Tlotleng · Melissa A. Vetten ·  
Frankline K. Keter · Amanda Skepu ·  
Robert Tshikhudo · Mary Gulumian

Received: 19 January 2016 / Accepted: 4 May 2016 / Published online: 16 May 2016  
© Springer Science+Business Media Dordrecht 2016

**Abstract** Surface-modified gold nanoparticles (AuNPs) are nanomaterials that hold promise in drug delivery applications. In this study, the cytotoxicity, uptake, intracellular localization, and the exocytosis of citrate-stabilized (Cit-AuNP) and polyethylene glycol (PEG)-modified gold nanoparticles with the carboxyl (COOH) terminal functional group were assessed in human embryonic kidney (HEK 293) and the human caucasian hepatocytes carcinoma (Hep G2) cell systems, representing two major accumulation sites for AuNPs. The zeta ( $\zeta$ )-potential measurements confirmed the negative surface charge of the AuNPs in water and in cell growth medium. The transmission electron microscopy confirmed the size and morphology of the AuNPs. Both types of AuNPs were shown to induce cytotoxic effects in cells. The Hep G2 cells were more sensitive cell type, with the COOH-PEG-AuNPs inducing the highest toxicity at higher concentrations. Dark field microscopy and TEM

images revealed that the AuNPs were internalized in cells, mostly as agglomerates. TEM micrographs further revealed that the AuNPs were confined as agglomerates inside vesicle-like compartments, likely to be endosomal and lysosomal structures as well as in the cytosol, mostly as individual particles. The AuNPs were shown to remain in cellular compartments for up to 3 weeks, but thereafter, clearance of the gold nanoparticles from the cells by exocytosis was evident. The results presented in this study may therefore give an indication on the fate of AuNPs on long-term exposure to cells and may also assist in safety evaluation of AuNPs.

**Keywords** Cytotoxicity · Exocytosis · Gold nanoparticles · Subcellular localization · Transmission electron microscopy · Uptake

## Background

The last decade has seen an increase in nanotechnology research with the development of nanomaterials for a wide range of medical applications. Gold nanoparticles (AuNPs), in particular, have gained popularity in the development of biomedical products (Liang et al. 2010). The most recent application of AuNPs is in the area of diagnostics (Baptista et al. 2008), pathogen control (Pissuwan et al. 2010), drug delivery (Pissuwan et al. 2011), cancer detection (Sarah 2010), cancer treatment (Chen et al. 2008; Chithrani et al. 2009), and gene therapy (Rosi et al. 2006). This is due to the desirable physicochemical and optical properties of AuNPs. For

N. Tlotleng · M. A. Vetten · M. Gulumian  
School of Pathology, Department of Molecular Medicine and  
Haematology, University of the Witwatersrand, P/Bag 3,  
Wits 2050, South Africa

N. Tlotleng · M. A. Vetten · M. Gulumian (✉)  
Toxicology and Biochemistry Section, National Institute for  
Occupational Health, 25 Hospital Street, Constitutional Hill,  
Johannesburg 2000, South Africa  
e-mail: mary.gulumian@nioh.nhls.ac.za

F. K. Keter · A. Skepu · R. Tshikhudo  
DST/Mintek Nanotechnology Innovation Centre Advanced  
Materials Division, Mintek, Private Bag X3015, Randburg 2125,  
South Africa

instance, the surface plasmon resonance (SPR) band of gold provides easy detection of the AuNPs within cells, contributing to their role in enhancing biological imaging (Levy et al. 2010).

The high chemical stability of AuNPs and their narrow size control during synthesis, but most importantly the ease of their surface modification through functionalization, have generated a great interest in the drug research field (Tiwari et al. 2011). Surface functionalization increase the biocompatibility and cellular availability of AuNPs (Patra et al. 2010; Zhang et al. 2010; Basiruddin et al. 2010) such as the effective delivery of the anticancer drug (oxaliplatin) to lung cancer cells using carboxylated (-COOH) PEG-AuNPs (Brown et al. 2010).

Poly(ethylene glycol) (PEG) is a tethered hydrophilic, generally considered non-toxic polymer. Hetero-functionalized PEGylated AuNPs with a thiol group on one terminus and a reactive functional group on the other end have become popular where functionalization of nanoparticles through PEG spacers allow for flexibility in the attached molecule for efficient interactions of the nanoparticles with biological target (Shenoy et al. 2006; Shukla et al. 2006).

The preferred end groups for hetero-functional PEG gold nanoparticles include biotin, nitriloacetic acid [NTA], -COOH, hydroxyl (OH), and methoxy (-O-CH<sub>3</sub>) functional groups (Grubbs 2007). The presence of such terminal groups on the nanoparticle surface allows the conjugation of a variety of biomolecules such as Streptavidin protein currently applied in many areas of commercial diagnostics (Aslan et al. 2004).

Endocytosis has been shown to be the major route of uptake of nanoparticles by cells and therefore is an important process for the efficient targeting of the nanoparticles to the cells of interest and delivery of biomolecules such as drugs. Most in vitro and in vivo studies have also shown that nanoparticle accumulation in cells through endocytosis can influence and alter fundamental cell functions and in some instances even cause cell death (Donaldson and Stone 2003). For example, Li et al. (2005) showed that internalized nanoparticles may target organelles such as the mitochondria to cause oxidative stress or the nucleus which may directly or indirectly induce DNA damage.

While the process of endocytosis is important, the exocytosis of the nanoparticle is equally important and must be understood, as nanoparticles remaining in the cell for a longer period after exposure increases the

possibility of unintended chronic toxicity (Oh and Park 2014a). Thus, it is important to not only study uptake but also the exocytosis of the internalized nanoparticles from cells, to decisively confirm their long-term safety.

Whereas high molecular weight PEG imparts more stability to the nanoparticle, short-chain low molecular weight PEG (1500–5000 Da) are preferred as they offer sufficient surface coverage on the nanoparticle surface and improve aqueous solubility (Tiwari et al. 2011; Otsuka et al. 2003). The AuNPs used in this study were therefore stabilized with low molecular weight PEGs where the cytotoxicity of citrate-capped and COOH-PEG-AuNP in two major cell systems were assessed. In addition, the intracellular localization as well as the long-term fate and exocytosis of these AuNPs in these two cell models were investigated.

## Materials and methods

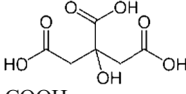
### Synthesis of AuNPs

The 14-nm AuNPs were prepared using the sodium citrate as the reducing agent as previously described (Turkevich et al. 1951). The gold (III) chloride trihydrate (HAuCl<sub>4</sub>·3H<sub>2</sub>O) and trisodium citrate (Na<sub>3</sub>C<sub>6</sub>H<sub>5</sub>O<sub>7</sub>·2H<sub>2</sub>O) were purchased from Sigma-Aldrich and used without further purification. Briefly, the 14-nm AuNPs were prepared by adding trisodium citrate aqueous solution (10 mL, 17 mM) into 180 mL (0.3 mM) of boiling HAuCl<sub>4</sub>·3H<sub>2</sub>O aqueous solution. The mixture was boiled under reflux for 15 min, and the resultant suspension was allowed to cool to room temperature.

The deep red citrate-capped gold nanoparticle suspension was further stirred overnight followed by filtration using a non-pyrogenic 0.25- $\mu$ m sterile filter before use. The COOH-PEG-AuNPs were prepared using ligand exchange procedures where the citrate was replaced with PEG-COOH. The ligand exchange experiments were left to run for about 8 h before being purified by centrifugation. The chemical description of AuNPs that were used in this study is presented in Table 1.

Before use, the AuNPs were tested for sterility, by placing a drop of the AuNP solution on tryptic soy agar plates. The plates were incubated for 2 to 7 days at 37 °C and inspected for bacterial and fungal growth. The absence of colonies (bacterial and fungal) confirmed the sterility of the samples.

**Table 1** Chemical description of the AuNPs used in the study

Name	Ligand type	Functional group	Molecular weight of ligand
Cit-AuNPs	2-Hydroxypropane-1,2,3-tricarboxylic acid Spacer: C11(EG)6		225.10
COOH-PEG-AuNPs	HS-PEG-Carboxyl Spacer: C11(EG)6	COOH	526.73

### Physicochemical characterization of the gold nanoparticles

The physicochemical properties (size and morphology, optical absorbance, hydrodynamic diameter, and the zeta potential) of the AuNPs suspended in Milli-Q water and in cell growth media were determined using TEM, Ultra-violet (UV-Vis) spectrophotometer, and dynamic light scattering (DLS), respectively. DLS measures Brownian motion and thus provided the overall size distribution of single as well as clustered particles in solution.

The AuNP samples were prepared for FTIR analysis according to the method of Zhou et al. (2010). Briefly the concentrated AuNP solution was centrifuged at  $13,000\times g$  for 30 min, the supernatant was discarded, and the pellet was dried for +12 h in a  $50^\circ\text{C}$  oven to remove the excess liquid. The pellet was mounted on the sample holder of the IR and the spectra were recorded. The instrument was operated in the absorbance mode at a resolution of  $6\text{ cm}^{-1}$ . To obtain a good signal to noise ratio, 64 scans were taken in the range of  $450\text{--}4500\text{ cm}^{-1}$ .

For characterization of the AuNPs in the cell culture media, the stock solution was centrifuged at  $13,000\times g$  for 30 min. The supernatant (buffer or water) was removed, and the pellet containing the AuNPs was resuspended in the culture media at the desired concentration. TEM images were acquired with a field emission JOEL-JEM 1010, operating at 120 kV. The absorbance of the AuNPs was determined on the Thermo Scientific Multiskan GO spectrophotometer. Zeta potential ( $\zeta$ -potential) measurements were performed using DLS technique.

### Toxicity studies

#### Cell cultures

The HEK 293 cells provided by Dr. Ely Abdullah from the Department of Molecular Medicine and

Haematology at the University of the Witwatersrand were maintained in Roswell Park Memorial Institute (RPMI)-1640 medium with L-glutamine, 10 % fetal bovine serum (FBS), and 1 % penicillin/streptomycin. The Hep G2 cell line was purchased from the European Collection of Cell Cultures (ECCAC, UK) and was maintained in Eagles minimum essential medium (EMEM) with L-glutamine supplemented with 10 % FBS and 1 % penicillin/streptomycin solution.

Both cell lines were kept at  $37^\circ\text{C}$  in a humidified 5 %  $\text{CO}_2$  and 95 % air atmosphere and were routinely tested for mycoplasma contamination using the MycoAlert<sup>®</sup> mycoplasma detection kit (Lonza, South Africa). The cells were grown in a  $75\text{-cm}^2$  tissue-culture flask. After reaching 80 % confluence, the cell monolayer was washed with phosphate-buffered saline (PBS) and detached from the flasks by a brief treatment with  $1\times$  trypsin/EDTA. The cells were resuspended in their respective growth medium. The cell viability was determined by the trypan blue cell viability assay and the cell number determined using a countess cell counter.

#### Cytotoxicity measurement

The impedance technology system xCELLigence<sup>™</sup> real-time cell analyzer (RTCA) instrument from ACEA Biosciences with RTCA software (version 1.2) was used in this study to measure cytotoxicity. The technology has previously been applied to monitor viability and proliferation of cells in vitro and to determine the dose-dependent response of different test substances (Atienza et al. 2006; Ürcan et al. 2010; Vetten et al. 2013).

For the present experiments, the HEK 293 and Hep G2 cells were seeded in a 96-well sensor electrode plate (E-plate) at  $5\times 10^4$  and  $1\times 10^4$  cells/per well, respectively. The E-plates for growing Hep G2 cells were pre-coated with poly-L-lysine (Sigma-Aldrich, South

Africa) as per manufacturer's recommendation to improve cell attachment.

The background reading was performed in the presence of 50  $\mu\text{L}$  of medium and in the absence of cells. Thereafter, the appropriate number of cells in 100  $\mu\text{L}$  of culture medium was added to each well to obtain the appropriate cell density. The E-plates containing the cells were allowed to incubate at room temperature for 30 min in a laminar flow cabinet prior to being placed in the E-Plate RTCA SP station in the incubator for real-time recording of impedance.

Cells were allowed to proliferate for 24 h prior to treatment with AuNPs, during which time the proliferation scan of the cells was acquired every 10 min. The cells were then treated with the AuNPs at final concentrations of 0.5, 1, 2, and 5 nM and returned to the incubator for further impedance reading, and their proliferation and dose response to the AuNPs were monitored. The information about the response of the cells was given as the cell index (CI) which reflects the viability of the treated cells over time. The CI scans was acquired every minute for 2 h and then every 15 min for the remainder of the experiment.

#### Uptake studies

##### *Cellular nanoparticle uptake of AuNPs using dark field imaging*

The intracellular uptake of AuNPs was assessed using a high-resolution illumination microscopy system (CytoViva Inc., Auburn, AL, USA). Briefly, HEK 293 and Hep G2 cells were grown at a cell density of  $7.4 \times 10^4$  cells/cm<sup>2</sup> overnight on clean autoclaved coverslips on a 12-well cell culture plate. The AuNPs were resuspended in cell culture media as previously described and introduced to the cells. The cells were incubated for 24 h at 37 °C to allow uptake of AuNPs by cells. The media were removed from the well, and the coverslips containing the cell monolayer were rinsed in PBS. The cells were fixed in 4 % formaldehyde-Tris/HCl buffer (pH 7.0) solution for 15 min at 4 °C.

Subsequently, the coverslips were rinsed with PBS and allowed to dry in the biosafety cabinet for 15 min before affixing with Kaiser's gelatine (Sigma-Aldrich, South Africa) onto glass slides for viewing. Dark-field images of the cells were captured at  $\times 60$  magnification using the CytoViva 150 Unit integrated onto the

Olympus BX43 microscope. Images were acquired using a DageXcel X16 camera.

##### *Subcellular localization of AuNPs with TEM*

TEM among other techniques has facilitated the detection of metal nanoparticles inside cells. AuNPs in particular are easily detected in cellular compartments because of the good contrast provided by their high density (Ng et al. 2010). In the present study, the uptake of the AuNPs in cells and their subcellular localization were verified with the analysis of ultrathin sections of cells.

Briefly, the cells were grown in 25-cm<sup>2</sup> cell culture flasks and were allowed to reach a confluency of about 60 % before exposure to the AuNPs. After 24 h of incubation, the medium was removed from the flask and the cell monolayer was washed and detached from the cell culture dish as previously described. The cell pellets were fixed in glutaraldehyde/formaldehyde solution in 0.1 M PBS (pH 7.4) at room temperature for 1 h. The cell suspension was centrifuged at  $10,397 \times g$  for 10 min. The glutaraldehyde fixative solution was removed, and the cell pellet was fixed in fresh fixative media overnight. After centrifugation, the pellet was washed three times in PBS and post-fixed with 1 % osmium tetroxide for 1 h, at room temperature.

The post-fixed cell pellets were sequentially dehydrated in ethanol (30, 50, 70, 80, 90, and 100 %) and then in propylene oxide before being transferred to BEEM capsules filled with epon resin. The capsules were incubated in a 60 °C oven for 48 h, to complete the embedding. Ultrathin sections (60–100 nm) were prepared with a Reichert Ultracut S microtome and transferred without any additional staining onto formvar-coated and non-coated copper grids.

The cellular materials on the copper grids were viewed with a field emission TEM (JEOL-JEM 2100F, Tokyo, Japan), fitted with an energy-dispersive X-ray spectrometer (EDS Oxford INCA spectrometer) and a digital Gatan camera (Erlangshen ES500 W). Cell sections on the non-coated copper grids were observed with the JEOL 100S TEM operated with an accelerating voltage of 80 kV. Energy-dispersive X-ray (EDX, EDAX system) spectra were taken at distinct points to determine the elemental composition of the internalized nanomaterial. Chemicals and materials that were used for TEM cell preparation were purchased from Agar Scientific, South Africa.

## Exocytosis studies

To assess exocytosis of the AuNPs, the Cit-AuNPs and the COOH-PEG-AuNPs were incubated with cells for 48 h (24 h post-treatment with AuNPs), 1 week (144 h post-treatment with AuNPs), 2 weeks (312 h post-treatment with AuNPs), 3 weeks (480 h post-treatment), and 4 weeks (648 h post-treatment with AuNPs). Following each incubation period, the medium was removed from the cell monolayer and analyzed for the presence of AuNPs using dark field microscope. The cell pellets were processed for TEM analysis as described previously.

## Statistical analysis for cytotoxicity studies

The slope for each curve of the normalized CI for the time period between treatment point and the highest CI value, i.e., confluency, of the untreated cells was calculated. The calculated slopes were exported to an excel sheet. The two sample *F* tests (*Fischer's test*) and the two sample *student's t* tests using the QI Macros software 2014 were used to compare if the differences between treated and untreated slopes were significant. Differences were considered statistically significant if  $p < 0.01$  and  $p > 0.05$  were considered non-significant.

## Results

FTIR spectrophotometry results revealed structural confirmation of the functional groups on the AuNP surfaces. The prominent peaks for the citrate-stabilized AuNPs as indicated in Fig. 1a were stretching frequencies of strong vibrations around  $2987.48$ ,  $2901.20$   $\text{cm}^{-1}$  ( $\nu$  (*O-H*)*s*), and  $1393.93$   $\text{cm}^{-1}$  ( $\nu$  (*O-H*)*m*), characteristic of the carboxylic acid of the citrate stabilizer. Following place exchange reaction, vibration frequencies at  $1760$   $\text{cm}^{-1}$  ( $\nu$  (*C=O*)*s*) were observed (Fig. 1b), characteristics of the carboxyl functional groups on the COOH-PEG-AuNPs.

Table 2 gives a summary of the physicochemical properties of the AuNPs in Milli-Q water and in cell growth media. A significantly large increase in the hydrodynamic size of the Cit-AuNPs and the COOH-PEG-AuNPs was seen when they were suspended in culture media. The average size of the Cit-AuNPs was increased from  $15 \pm 2$  nm when suspended in water to 38 nm when suspended in RPMI-1640 medium and to

46 nm when suspended in EMEM medium. Similarly, the size of the COOH-PEG-AuNPs was increased from  $15 \pm 3$  to 39 nm when suspended in RPMI-1640 medium and to 80 nm when suspended in EMEM medium.

The particle size increase suggests agglomeration of the nanoparticles, possibly due to the presence of adsorbed medium components on the gold nanoparticle surfaces (Lacerda et al. 2010; Navya and Daima 2016). As previously described, DLS data report the average hydrodynamic size representing any adsorbed material on the nanoparticle surface as well as the hydrodynamic diameter of the particles (Graf et al. 2012). Hence, the overestimation in the mean particle size diameters in DLS measurements is attributed to the high scattering intensities of larger nanoparticles (Albanese and Chan 2011).

The surface charge (zeta potential) of the AuNPs in water and in cell growth media was measured to further analyze the degree of stability of the nanoparticles. The measurements were made in triplicate, and the average values are shown in Table 2. Zeta potential analyses in water show values of  $-38.5$  and  $-46.2$  mV for Cit-AuNPs and COOH-PEG AuNPs, respectively, indicating extreme stability of negatively charged AuNPs in water (Sabuncu et al. 2012). However, upon resuspending in cell culture medium, the zeta potential values were decreased with no significant difference in the zeta potential readings of the two AuNPs in the two growth media. The zeta potential of colloids has been shown to decrease in physiological media, including cell growth medium where it is indicated that the observed decrease in zeta potential and the instability of the nanoparticles may be due to the increased ionic strength of the media (Sabuncu et al. 2012).

The UV-Vis absorption measurements of the AuNPs are also presented in Table 2. The optical spectrum of the synthesized Cit-AuNPs in water was 519 nm, which is in agreement with the SPR absorption of nanosized AuNPs at this size range reported in the literature (Jain et al. 2006). Upon suspending in cell growth medium, the SPR spectra for the Cit-AuNPs were shifted to 557 and 544 nm for RPMI and EMEM, respectively. The red shift has been observed in the measured spectra of AuNPs in biological medium and is attributed, once again, to the formation of agglomerates and to the formation of protein corona (Albanese and Chan 2011; Maiorano et al. 2010). A similar shift in the plasmon absorption was also observed with the COOH-PEG-AuNPs where the optical spectrum of 522 nm measured

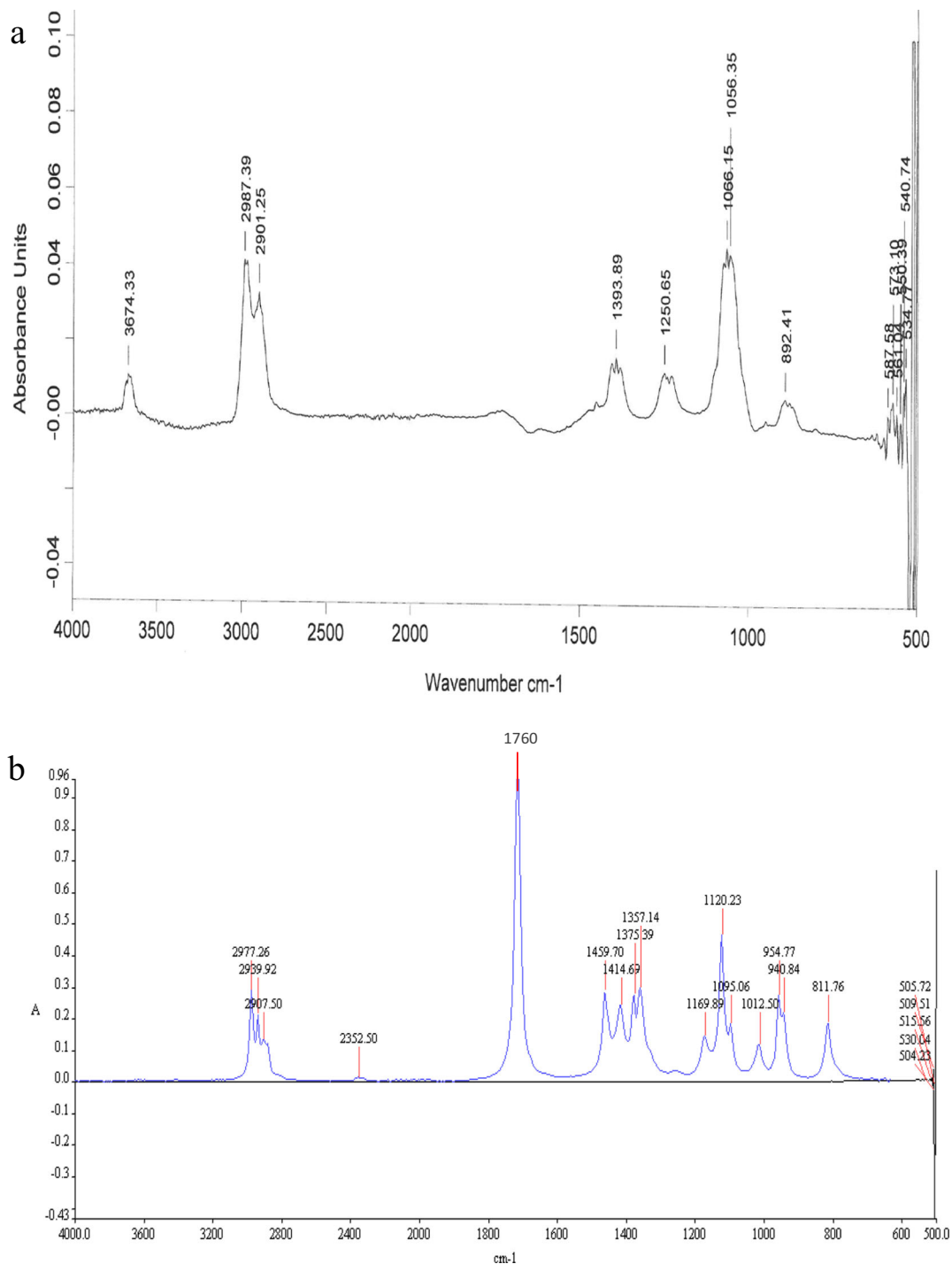


**Fig. 1** FTIR spectra of citrate stabilized (a) and COOH-PEG AuNPs (b), indicating vibration frequencies of  $2972.50\text{ cm}^{-1}$  ( $\nu(O-H)s$ ),  $2907.50\text{ cm}^{-1}$  ( $\nu(C-H)m$ ),

$1394.20\text{ cm}^{-1}$  ( $\nu(C-H)m$ ), and  $1760\text{ cm}^{-1}$  ( $\nu(C=O)s$ ) characteristics of the carboxylic acid of the citrate stabilizer and carboxyl functional groups in COOH-PEG AuNPs

in water was increased to 538 nm in RPMI-1640 and to 542 nm in EMEM growth medium indicating

agglomeration. The formation of such agglomeration for the two AuNP samples could be further confirmed

**Table 2** Physicochemical properties of AuNPs in Milli-Q water and in cell growth media

AuNP	Hydrodynamic average size by DLS (nm)			$\zeta$ -potential (mV)			UV-Vis ( $\lambda$ nm)			pH at 37 °C		
	Water	RPMI	EMEM	Water	RPMI	EMEM	Water	RPMI	EMEM	Water	RPMI	EMEM
Cit-AuNPs	15.2	37.8	46.2	-38.5	-10.1	-8.9	519	557	544	6.2	7.61	7.8
COOH-PEG AuNPs	15.30	39.5	80.4	-46.2	-7.1	-7.7	520	538	543	6.8	7.65	7.8

with TEM images presented in Fig. 2a, b with their corresponding full spectra and size distribution of an average of 16 nm for the Cit-AuNPs and 22 nm for the COOH-PEG-AuNPs.

### Cytotoxicity measurement of AuNPs

The cytotoxicity of the AuNPs was determined in HEK 293 cells using label-free real-time cell analyzer impedance technology. Figure 3 shows the proliferation curves of HEK 293 cells that were treated with Cit-AuNPs (Fig. 3a) and COOH-PEG-AuNPs (Fig. 3b) for a period of 56 h (32 h post-treatment).

Figure 3a demonstrates that treatment with Cit-AuNPs decreased the viability in HEK 293 cells at the tested concentrations. The cell index of the treated cells began to deviate from the control at approximately 8 h and was found to significantly lower after 22 h ( $p < 0.05$ ). The presence of citrate ions on the Cit-AuNP surfaces have been correlated to the observed toxicity associated with these particles (Uboldi et al. 2009). Figure 3b shows the proliferation curves of HEK 293 cells that were treated with the COOH-PEG-AuNPs. A cytotoxic response was seen with cells at all four selected concentrations ( $p < 0.01$  for 5, 2, 1 nM;  $p < 0.05$  for 0.5 nM), in a concentration-dependent manner. The viability of the cells was therefore affected by the COOH-PEG-AuNPs, as the cell index remained lower than the control throughout the test.

Figure 4 shows the proliferation curves of Hep G2 cells treated with 14-nm Cit-AuNPs (Fig. 4a) and COOH-PEG-AuNPs (Fig. 4b) for a period of 98 h (74 h post-treatment with the gold nanoparticles).

The figure demonstrates that treatment with Cit-AuNPs significantly reduced the viability of Hep G2 cells ( $p < 0.01$ ), indicating that the Cit-AuNPs were cytotoxic to Hep G2 cells at the tested concentrations. The decrease in cell viability was evident within a few hours

after the addition of the nanoparticles to Hep G2 cells and remained lower than the control for the duration of the experiment.

A concentration-dependent response was also seen in cells treated with COOH-PEG-AuNPs (Fig. 4b). Highest tested concentration of 5 nM ( $p < 0.01$ ) and 2 nM ( $p < 0.01$ ) reduced the viability of cells to zero immediately after the addition of the nanoparticles indicating that no viable cells remained attached to the microelectrode plate. On the other hand, the COOH-PEG-AuNPs did not show any cytotoxic effect to Hep G2 cells at lower concentrations of 0.5 nM ( $p > 0.05$ ) and 1 nM AuNPs ( $p > 0.05$ ) where the viability of the treated cells was similar to those of the control untreated cells.

### Cellular uptake

Using dark field microscopy combined with a visible and near-infrared (VNIR) hyperspectral imaging system, uptake of the AuNPs by the cells was studied. Although this technology does not provide comprehensive information on the localization of the AuNPs in cells, the hyperspectral imaging system has been suggested as a simple and convenient technique to visualize cellular uptake and also to characterize the extent of aggregation of the internalized nanoparticles (Skebo et al. 2007; Rocha et al. 2011; Vetten et al. 2013). Figure 5 shows dark field images of HEK 293 and Hep G2 cells after incubation with the AuNPs where the nanoparticles were distinguished in the images as bright figures resulting from their intense light-scattering ability. The hyperspectral profiles of the AuNPs, confirming intracellular nanoparticles, are shown in Fig. 5e, f.

Figures 5a, c shows images of HEK 293 and Hep G2 cells, respectively, that were incubated with the Cit-AuNPs. The images showed that the majority of the Cit-

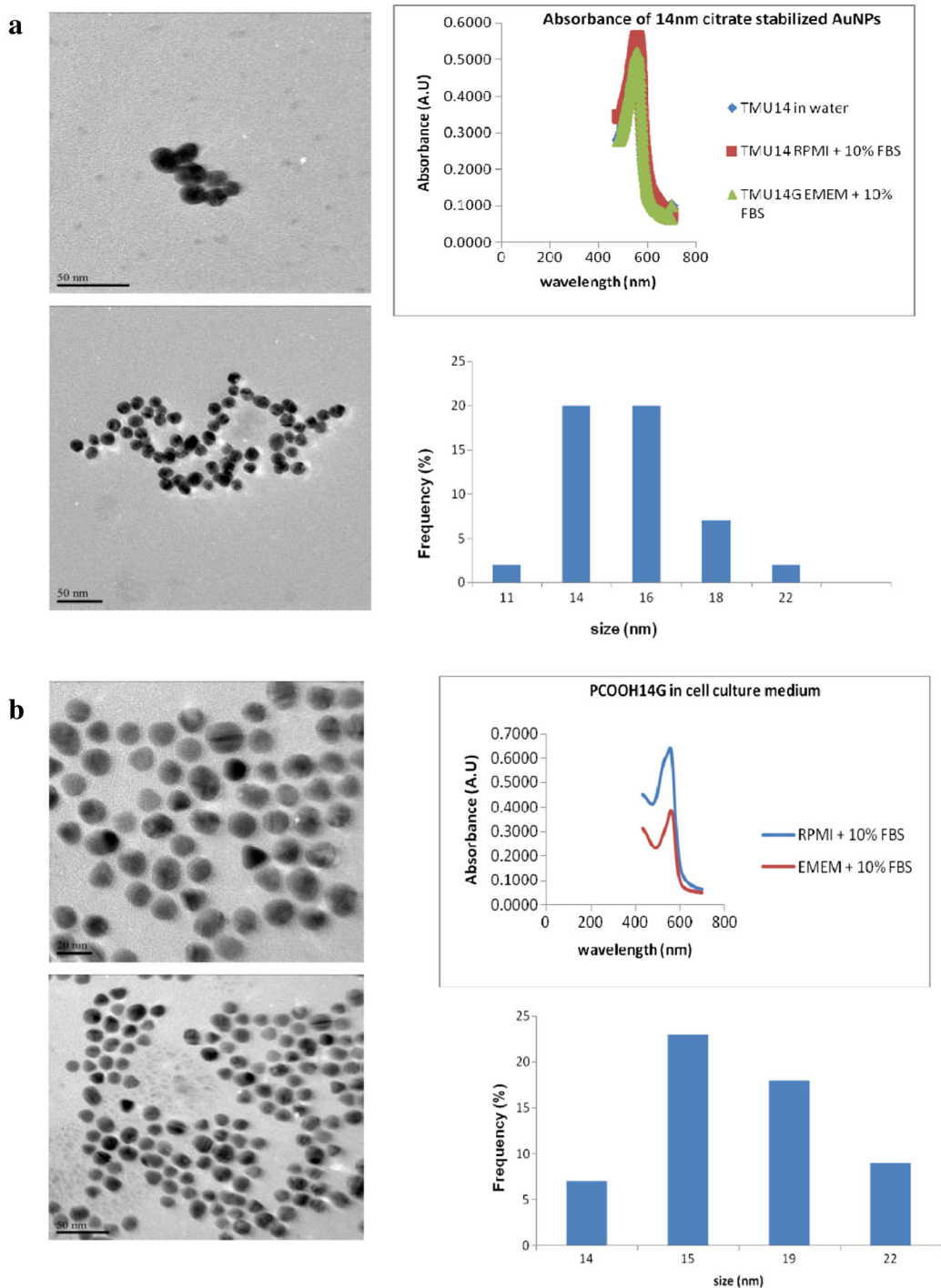


**Fig. 2** TEM images and size distribution analysis of **a** 14 nm Cit-AuNPs and **b** COOH-PEG-AuNPs in RPMI-1640 (*top image in a and b*) and EMEM (*bottom image in a and b*)

AuNPs were internalized by cells. However, images of cells that were incubated with the COOH-PEG AuNPs shown in Fig. 5b, d demonstrated that the majority of these

particles were accumulated on the cell membranes, mainly as agglomerates. Nonetheless, a small number of these particles were also visible inside the cells.



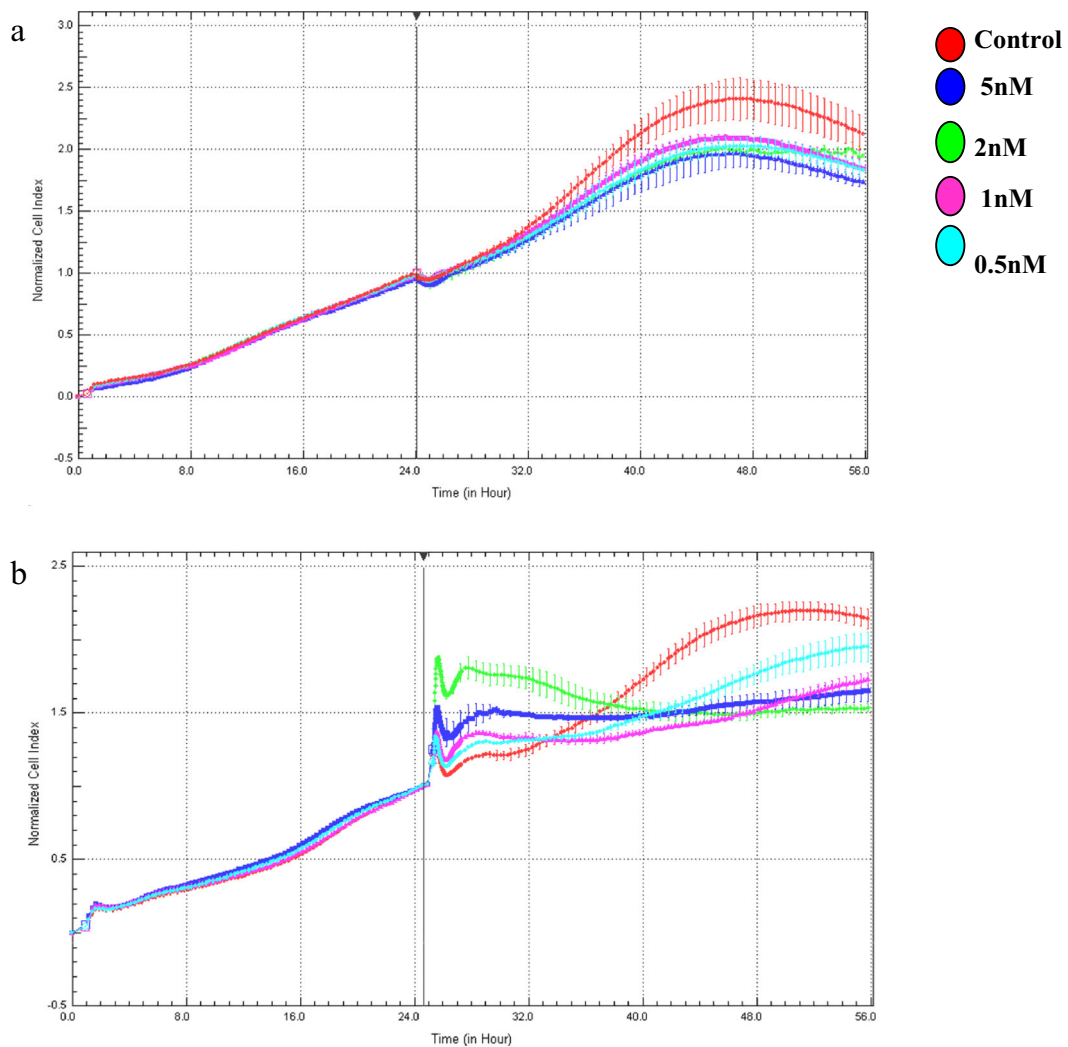


**Fig. 3** Impedance monitoring of proliferation in HEK 293 cells following 56 h incubation with 14-nm citrate-stabilized AuNPs at concentrations of 5, 2, 1, and 0.5 nM. **a** 14 nm Cit-AuNPs and **b** 14 nm COOH-PEG-AuNPs

### Uptake and subcellular localization

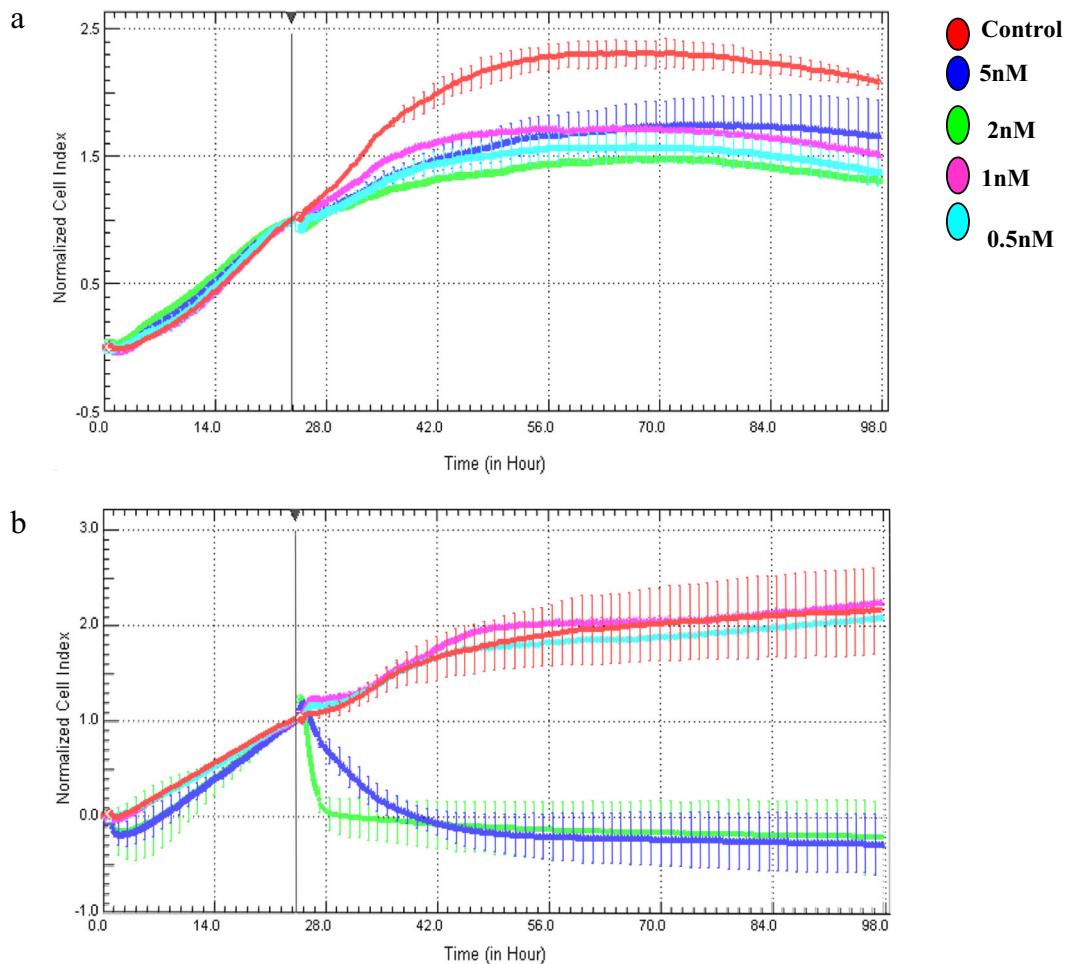
TEM images were used to confirm AuNP uptake into the cells as well as to assess their intracellular distribution and localization in different cellular compartments. As seen in Fig. 6, the Cit-AuNPs were taken up by HEK 293 cells and accumulated inside the cells as agglomerates of different sizes.

Figure 6a shows that the Cit-AuNPs were dispersed in the cytoplasm of HEK 293 cells while in Hep G2 cells the Cit-AuNPs were confined in large cellular vesicles, again mainly as agglomerates (Fig. 6b). Figure 6b also shows that Cit-AuNPs are attached to the cell membrane of Hep G2 cells, possibly during entry into the cells. Intracellular AuNPs were confirmed by EDX analysis

(Fig. 6c) which revealed a significant Au peak at 2.3 keV in cell samples that were exposed to the Cit-AuNPs.

The images in Fig. 7 show internalized COOH-PEG-AuNPs in cells.

Figure 7a, b shows that the COOH-PEG-AuNPs were localized in the cell cytoplasm of HEK 293 cells and in cellular vesicles, most likely to be the recycling endosomal vesicles (indicated by arrows). COOH-PEG-AuNPs were deposited in HEK 293 cells as single as well as agglomerated particles of different sizes. Figure 7c, d shows COOH-PEG-AuNPs in Hep G2 cells. The AuNPs were deposited in Hep G2 cells as individual and agglomerated particles in the cytoplasm (indicated by circles). Some of the COOH-PEG-AuNPs



**Fig. 4** Impedance monitoring of proliferation in Hep G2 cells following 98 h incubation with AuNPs concentrations of 5, 2, 1, and 0.5 nM. **a** 14 nm Cit-AuNPs and **b** 14 nm COOH-PEG-AuNPs

were seen in invaginated areas of the cell plasma membrane of Hep G2 cells (Fig. 7c). The EDX spectrum confirming intracellular COOH-PEG-AuNPs in cells is shown in Fig. 7e.

#### Cellular exocytosis of AuNPs

Following uptake of AuNPs into cells, experiments were conducted to investigate their intracellular fate. The HEK 293 and Hep G2 cells were therefore treated with the nanoparticles for 24 h, and the medium containing the AuNP was removed. The cells were then incubated with fresh medium containing no particles for an additional 48 h, 1 week, 2 weeks, 3 weeks, and 4 weeks.

Representative TEM images of HEK 293 cells incubated with Cit-AuNPs and COOH-PEG-AuNPs are

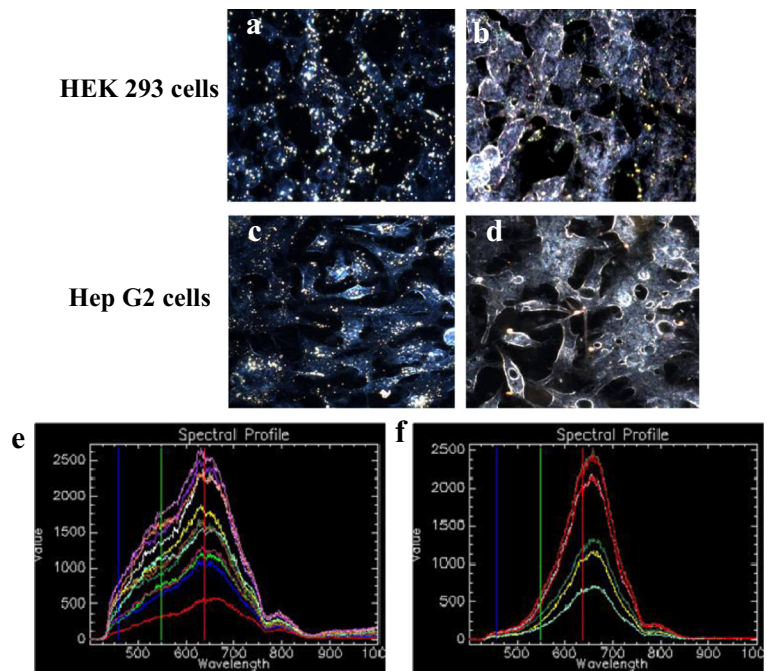
shown in Fig. 8, where the uptake was much higher with Cit-AuNPs (Fig. 8a–d) compared to COOH-PEG-AuNPs (Fig. 8e–h).

Moreover, after 48 h and up to 3 weeks of incubation, the majority of the Cit-AuNPs (Fig. 8a–d) and a fraction of COOH-AuNPs (Fig. 8e–h) were seen in vesicles of HEK 293 cells with the observation that some of the Cit-AuNPs were also deposited in the cell cytoplasm (Fig. 8b–d). Nonetheless, there were no particles inside the cells after 4 weeks of incubation (results not shown).

Similar observations were also seen with Hep G2 cells incubated with Cit-AuNPs (Fig. 9a–d), where the Cit-AuNPs in vesicles of Hep G2 cells were eventually depleted from cells after 4 weeks of culture through excretion to the extracellular medium (Fig. 9e, f).

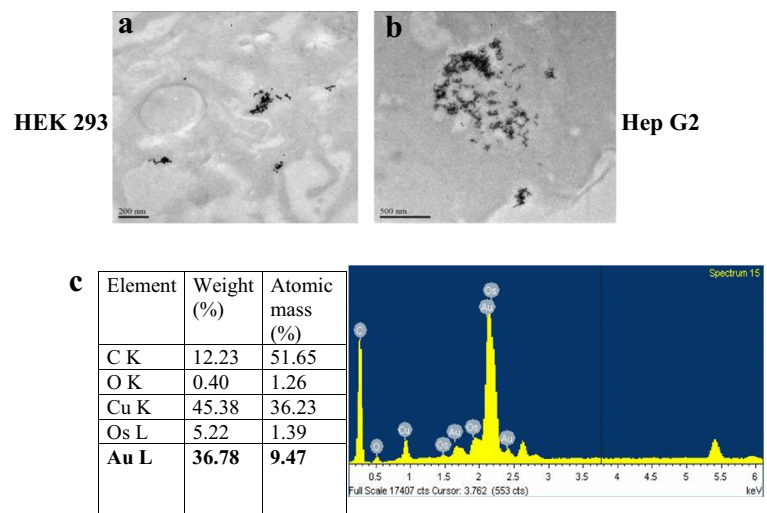
Figure 10 shows TEM images of Hep G2 incubated with COOH-PEG-AuNPs. The images show the

**Fig. 5** Uptake of AuNPs by HEK 293 (a, b) and Hep G2 (c, d) cells observed with a dark field microscopy. Cells were incubated for 24 h with 14-nm citrate-capped AuNPs (a, c) and COOH-PEG-AuNPs (b, d) before observation with high-resolution illumination microscopy. AuNPs were visible as bright spectra associated with cells at  $\times 60$  magnification. Hyperspectral image of citrate-AuNPs (e) and COOH-PEG-AuNPs (f) showing a cross-sectional scan of randomly selected individual or aggregated nanoparticles



COOH-PEG-AuNPs in vesicles of Hep G2 cells 48 h, 1 week, and 2 weeks after culture (Figures 10a and 9d). Ultrathin sections of cells showed that COOH-PEG-AuNPs about to be removed from the cells are localized close to the cell membrane 1 week after culture (Fig. 10c). Exocytosis by vesicle secretion (Fig. 10e) and non-vesicle secretion (Fig. 10f) was evident in representative images of Hep G2 that were incubated with COOH-PEG-AuNPs for 3 and 4 weeks, respectively (Fig. 10e, f).

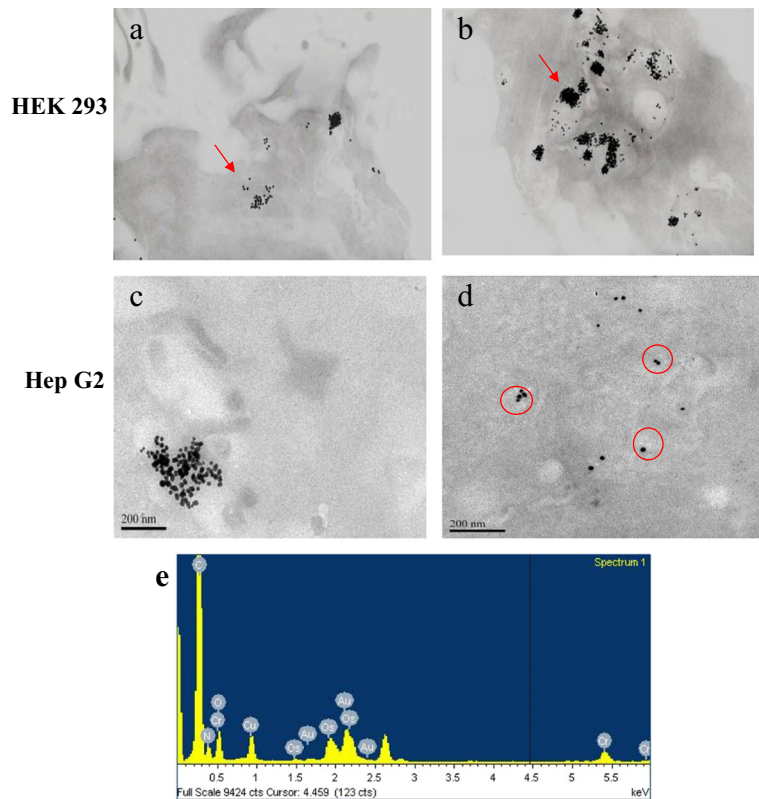
**Fig. 6** TEM images showing intracellular Cit-AuNPs in a HEK 293 and b Hep G2 cells. c Shows EDX spectra confirming the elemental Au in cell sections



To confirm the exocytosis of AuNPs to the extracellular media, the cell supernatant was analyzed for the presence of AuNPs using dark field imaging. Cell culture media that were collected at 24 h, 48 h, 1 week, 2 weeks, 3 weeks, and 4 weeks during incubation of Hep G2 cells with the AuNPs are shown in Fig. 11.

The images confirmed excreted nanoparticles in the medium as agglomerates of different sizes. Similar results were obtained in cell culture medium of HEK 293 cells (results not shown).

**Fig. 7** TEM images of HEK 293 (a, b) and Hep G2 (c, d) cells treated with COOH-PEG-AuNPs for 24 h. Scale bar: 500 nm. Arrows in Fig. 6b indicate cellular vesicles containing singular and agglomerated COOH-PEG-AuNPs. The red circles in Fig. 6d indicate freely dispersed AuNPs in the cytoplasm of Hep G2 cells. e EDX spectra of Au in cell sections (color figure online)



## Discussion

In this study, we have assessed the toxicity, uptake, intracellular localization, and exocytosis of Cit-AuNPs and COOH-PEG AuNPs. Toxicity studies were first conducted where our findings showed a statistically significant effect by both Cit-AuNPs and COOH-PEG AuNPs in all tested concentrations on HEK 293 and Hep G2 cells. Such cell-specific differences in toxicity of AuNPs have previously been confirmed in our laboratory (Vetten et al. 2013).

The present cytotoxicity studies have shown that the Cit-AuNPs decreased the viability of HEK 293 cells about 22 h, while cytotoxicity on Hep G2 cells was seen after a few hours upon addition of the AuNPs. In the literature, a number of studies were conducted to assess the cytotoxicity of citrate-stabilized AuNPs of similar size. For example, the cytotoxicity of 10- and 11-nm Cit-AuNPs at different concentrations to human dermal endothelial (HDMEC) and human cerebral endothelial (hCMEC/D3) cells exposed for 48 h was reported (Freese et al. 2012). On the other hand, non-cytotoxic

**Fig. 8** TEM image of HEK 293 cells incubated with Cit-AuNPs (a–d) and COOH-PEG-AuNPs (e–h) for (a, e) 48 h, (b, f) 1 week (c, g), 2 weeks (d, h), and 3 weeks (indicated by arrows)

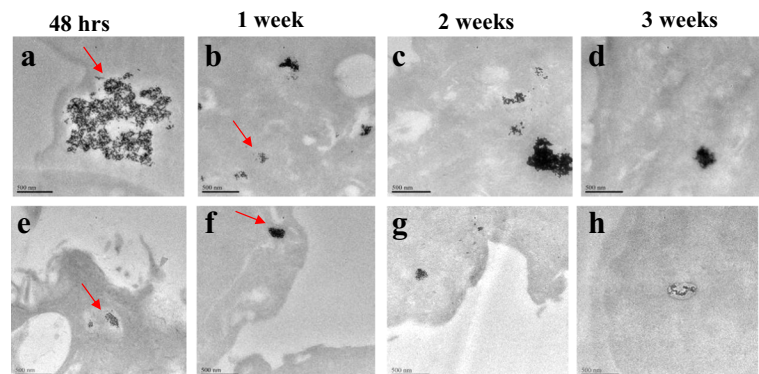
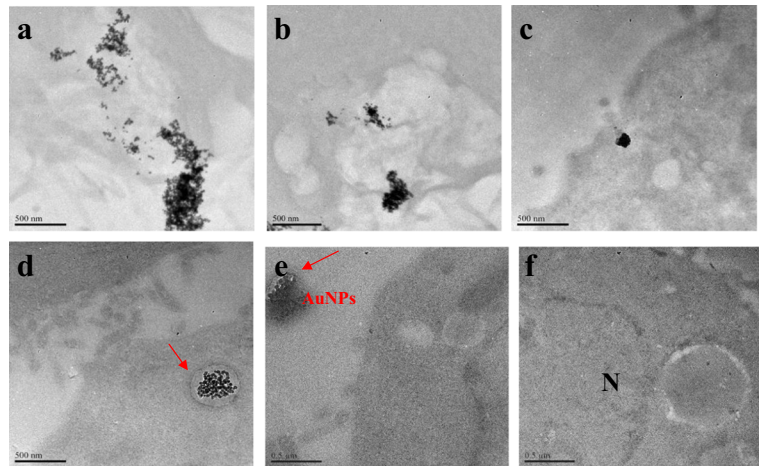


**Fig. 9** Representative image from TEM showing Hep G2 cells incubated with 14 nm Cit-AuNPs for **a** 48 h, **b** 1 week, **c** 2 weeks, **d** 3 weeks, and **e** and **f** 4 weeks (**f**)



effects, assessed by viability and membrane integrity, of 18-nm Cit-AuNPs to K562 leukemia cell line (Connor et al. 2005) and of 20 nm Cit-AuNPs to Hep G2 cells, assessed by cell viability and proliferation (Fraga et al. 2013), were reported.

In addition, our findings have shown that at lower concentrations, COOH-PEG AuNPs were non-toxic to Hep G2 cells while toxic to HEK 293 cells at all tested concentrations. The non-toxic nature of 2 nm COOH-PEG-AuNPs to Cos-1 mammalian cells, assessed by cell viability and proliferation, was also reported (Goodman et al. 2004).

The results presented in this study and those reported in the literature may therefore suggest that the differences observed in the cytotoxicity of Cit-AuNPs and COOH-PEG AuNPs will depend on the number of physicochemical properties including size and surface coating, as well as on type of cell studied (Li et al. 2015).

However, a closer scrutiny may suggest that the methodologies implemented to assess this toxicity may influence the outcome of the cytotoxicity results.

All those studies reported in the literature have implemented the absorbance-based XTT assay; in addition, they have used other assay systems that rely on photometric measurements (Freese et al. 2012; Connor et al. 2005; Goodman et al. 2004). As a result of the SPR properties, AuNPs are shown to potentially interfere with a number of *in vitro* toxicity assays that rely on photometric measurements. It is therefore recommended that in order to avoid such interference, alternative methods that do not rely on photometric measurements be employed (Vetten et al. 2013). Subsequently, the use of label-free impedance methodology, the xCELLigence RTCA system, in our study may have produced a more true reflection of cellular response to these nanoparticles.

**Fig. 10** TEM image of Hep G2 cells incubated with COOH-PEG-AuNPs for **a** 48 hrs, **b**, **c** 1 week, **d** 2 weeks, **e** 3 weeks, and **f** 4 weeks (the *arrows* in Fig. 9e, f are pointing at excreted AuNPs)

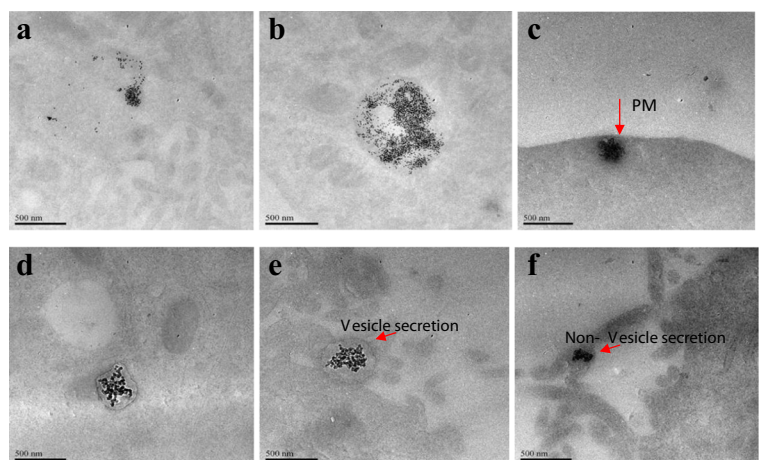
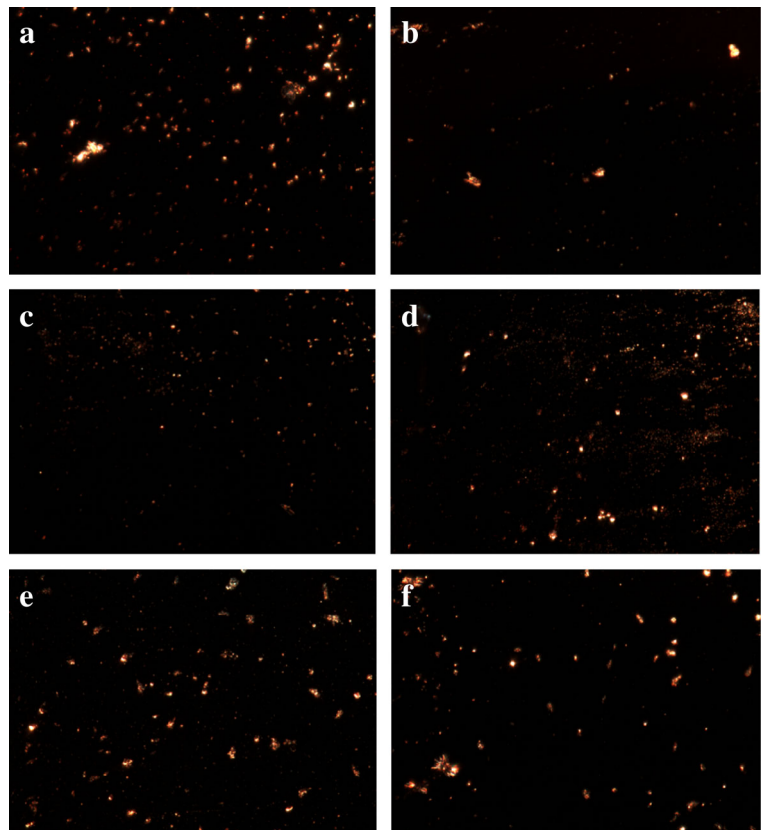


**Fig. 11** Cell growth medium of Hep G2 cells collected at **a** 24 h, **b** 48 h, **c** 1 week, **d** 2 weeks, **e** 3 weeks, and **f** 4 weeks period during which the cells were maintained



The present study has also assessed the uptake of AuNPs in cells using dark field microscopy. Results have indicated a high degree of internalization of Cit-AuNPs by both HEK 293 and Hep G2 cells confirming those reported in the literature with U937 cells (Oh and Park 2014b) and human alveolar epithelial (A549) cells (Brandenberger et al. 2010). The high uptake of Cit-AuNPs was proposed to be linked to the binding of serum proteins onto the citrate ions, thereby resulting in a higher concentration of Cit-AuNPs uptake into cells (Chithrani et al. 2009).

In addition, the present results have indicated that the majority of COOH-PEG-AuNPs were not internalized by HEK 293 and Hep G2 cells but rather have accumulated on the surface of these cells, which was confirmed with TEM imaging. These observations were confirmed in the literature for COOH-PEG-thioactic acid (TA)-AuNPs with kidney COS-1 cells (Oh et al. 2011) and for methoxy-PEG-AuNPs with U937 cells (Oh and Park 2014b). This was explained to be due to the hydrophilicity of the PEG molecule that has been shown to

contribute to the minimal uptake of PEG-coated AuNPs into cells (Kettler et al. 2014).

TEM images have further confirmed the intracellular uptake and in addition the subcellular localization of AuNPs in cells. Intracellular Cit-AuNPs were seen to exist as agglomerates of different sizes in HEK 293 and in Hep G2 cells 24 h after culture, the majority of which were localized in the cytoplasm of HEK 293 cells and in large vesicles, likely to be endosomes, of Hep G2 cells 24 h after incubation. Our observations were similar to those reported with HeLa cells (Nativo et al. 2008), macrophage RAW 264.7 cells (Liu et al. 2013), and Hep G2 cells (Chu et al. 2014).

Similarly, TEM images have indicated that COOH-PEG-AuNPs have localized in agglomerates in vesicles of different sizes in HEK 293 cells but also in the cell cytoplasm of both HEK 293 and Hep G2 cells. Most importantly, our results indicated that there was no evidence of nuclear or mitochondrial accumulation of Cit-AuNPs or COOH-PEG-AuNPs in the cells. Lack of localization of AuNPs in these cellular compartments

was reported for 14-, 50-, and 74-nm citrate-stabilized AuNPs in breast cancer (MCF-7) cells (Chithrani et al. 2009). However, it was shown that AuNPs with hydrodynamic size less than 5 nm were likely to gain access to the cell nucleus (Gu et al. 2009; Kim et al. 2015).

Finally, the exocytosis of the Cit-AuNPs and the COOH-PEG-AuNPs were investigated with TEM. The results have shown that the majority of the AuNPs were retained in both cell types for up to 3 weeks. The absence of AuNPs in cells after 4 weeks of culture has confirmed that the AuNPs were eventually cleared from cells. Additionally, dark field images of expelled AuNPs in cell medium suggested that they were removed from cells as agglomerates of different sizes. These observations were confirmed in the literature with 10-, 20, and 40-nm citrate-AuNPs and PEG-coated AuNPs in macrophage cells (Oh and Park 2014b).

The TEM results have indicated the exocytosis of Cit-AuNPs and COOH-PEG-AuNPs to be similar with that of Hep G2 where vesicles filled with these nanoparticles were excreted to the medium during exocytosis. Once again, the latter observations were confirmed for citrate and PEG-coated AuNPs in macrophages (Oh and Park 2014b). Spherical nanoparticles remaining in endosomes after endocytosis have been shown to be easily excreted by exocytosis when compared to nanoparticles of different morphologies (Chu et al. 2014).

In summary, this study has presented cytotoxic effects of Cit-AuNPs and COOH-PEG-AuNPs on two major cell lines, HEK 293 and Hep G2 cells. Cytotoxicity measurements with real-time impedance showed that both cell types were sensitive to the AuNPs, regardless of the surface chemistry on these nanoparticles; however, the COOH-PEG-AuNPs were more toxic, with higher levels of cytotoxicity observed in the Hep G2 cells than in HEK 293 cells. At concentrations with low toxicity, uptake was observed for both AuNPs, with higher uptake of Cit-AuNPs than that of the COOH-PEG-AuNPs. Nonetheless, intracellular localization of the AuNPs in cells did not depend on surface chemistry where majority of the AuNPs were localized in agglomerates within vesicles, which were exocytosed following longer incubations.

## Conclusions

These observations emphasize the importance of surface chemistry of AuNPs in the assessment of their uptake

and cellular compartmental distribution as well as in their fate through exocytosis in relation to their long-term effects. However, similar *in vivo* studies need to be conducted to confirm these *in vitro* observations as clearance of nanoparticles from cells prevents unintended toxicity associated with particles that have prolonged intracellular retention.

**Acknowledgments** This work is supported by the South African Department of Science and Technology (DST) and the National Research Foundation (NRF). The authors wish to thank Prof Jim Phillips from the Pathology Department at the National Institute for Occupational Health (NIOH) for the technical advice in preparing samples for TEM for assistance with acquiring the TEM images. We also thank the Immunology and Microbiology Department of the NIOH for sterility testing of the AuNPs.

**Authors' contributions** AuNPs were synthesized by FKK and AS. Characterization of the AuNPs was done by FKK and NT. xCELLigence, CytoViva, and TEM work was performed by NT. NT, MV, RT, and MG were involved in the inception and planning of the project and in the preparation of the manuscript. All authors read and approved the final manuscript.

## Compliance with ethical standards

**Competing interests** The authors declare that they have no competing interests.

## References

- Albanese A, Chan WCW. Effects of gold nanoparticle aggregation on cell uptake and toxicity. *ACS Nano*. 2011;5(7):5478–89.
- Aslan K, Luhrs CC, Perez-Luna VH. Controlled and reversible aggregation of biotinylated gold nanoparticles with Streptavidin. *J Phys Chem B*. 2004;108:1561–15639.
- Atienza JM, Yu N, Kirstein SL, Xi B, Wang X, Xu X, et al. Dynamic and label-free cell-based assays using the real-time cell electronic sensing system. *Assay Drug Dev Technol*. 2006;4:597–607.
- Baptista P, Pereira E, Eaton P, Doria G, Miranda A, Gomes I, et al. Gold nanoparticles for the development of clinical diagnostics methods. *Anal Bioanal Chem*. 2008;391:943–50.
- Basiruddin SK, Saha A, Pradhan N. Functionalized gold nanorod solution via reverse micelle based polyacrylate coating. *Langmuir*. 2010;26:7475–81.
- Brandenberger C, Clift MJD, Vanhecke D, Muhfeld C, Stone V, Rothen-Rutishauser B. Intracellular imaging of nanoparticles: is it an elemental mistake to believe what you see? *Part Fibre Toxicol*. 2010;7(15):1–6.
- Brown SD, Native P, Smith J, Stirling D, Edward PR, Venugopal B. Gold nanoparticles for the improved anticancer drug delivery of the active component of oxaliplatin. *J Am Chem Soc*. 2010;132:4679–89.

- Chen PC, Mwakwari SC, Oyelere AK. Gold nanoparticles: from medicine to nanosensing. *Nanotechnol Sci Appl*. 2008;1:45–66. 2008.
- Chithrani BD, Steward A, Allen C, Jaffary DA. Intracellular uptake, transport, and processing of nanostructures in cancer cells. *Nanomed Nanotechnol Biol Med*. 2009;5:8–127. 2009.
- Chu Z, Zhang S, Zhang B, Zhang C, Fang CY, Li Q. Unambiguous observation of shape effects on cellular fate of nanoparticles. *Sci Rep*. 2014;4(4495):1–9.
- Connor EE, Mwamuka J, Gole A, Murphy CJ, Wyatt MD. Gold nanoparticles are taken up by human cells but do not cause acute cytotoxicity. *Small*. 2005;1:325–7.
- Donaldson K, Stone V. Current hypothesis on the mechanisms of toxicity of ultrafine particles. *Ann Ist Super Sanita*. 2003;39(3):405–10.
- Fraga S, Faria H, Soares ME, Carmo H. Influence of the surface coating on the cytotoxicity, genotoxicity and uptake of gold nanoparticles in human HepG2 cells. *J Appl Toxicol*. 2013. doi:10.1002/jat.2865.
- Freese C, Uboldi C, Gibson MI, Unger RE, Weksler BB, Romero IA, et al. Uptake and cytotoxicity of citrate-coated gold nanospheres: comparative studies on human endothelial and epithelial cells. *Part Fibre Toxicol*. 2012;9(3):6–11.
- Goodman CM, McCusker CD, Yilmaz T, Rotello VM. Toxicity of gold nanoparticles functionalized with cationic and anionic side chains. *Bioconjug Chem*. 2004;15:897–900.
- Graf C, Gao Q, Schutz I, Noufele CN, Ruan W, Ruhl E. Surface functionalization of silica nanoparticles supports colloidal stability in physiological media and facilitates internalization in cells. *Langmuir*. 2012;28:7598–613.
- Grubbs RB. Roles of polymer ligands in nanoparticle stabilization. *Polym Rev*. 2007;47(2):197–215.
- Gu YJ, Cheng J, Lin CC, Lam YW, Cheng SH, Wong WT. Nuclear penetration of surface functionalized gold nanoparticles. *Toxicol Appl Pharmacol*. 2009;237:196–204.
- Jain PK, Lee KS, El-Sayed IH, El-Sayed MA. Calculated Absorption and scattering properties of gold nanoparticles of different size, shape, and composition: applications in biological imaging and biomedicine. *J Phys Chem B*. 2006;110:7238–48.
- Kettler K, Veltman K, Van De Meent D, Van Wzel A, Hendriks AJ. Cellular uptake of nanoparticles as determined by particle properties, experimental conditions and cell type. *Environ Toxicol Chem*. 2014;33(3):481–92.
- Kim CS, Li X, Jiang Y, Yan B, Tonga GY, Ray M, et al. Cellular imaging of endosome entrapped small gold nanoparticles. *MethodsX*. 2015;2:306–15.
- Lacerda SH, Park JJ, Meuse C, Pristiniski D, Becker ML, Douglas JF. Interaction of gold nanoparticles with common human blood proteins. *ACS Nano*. 2010;4(1):365–79.
- Levy R, Shaheen U, Cesbron Y, See V. Gold nanoparticle delivery in mammalian live cells: a critical review. *Nano Rev*. 2010;1:4889–94.
- Li JJ, Zou LI, Hartono D, Ong EN, Bay BH, Yung LL. Gold nanoparticles induce oxidative damage in lung fibroblasts: in vitro. *Adv Mater*. 2005;20:138–42.
- Li X, Liu W, Sun L, Aifantis KE, Yu B, Fan Y, et al. Effects of physicochemical properties of nanomaterials on their toxicity. *J Biomed Mater Res Part A*. 2015;103A:2499–507.
- Liang M, Lin C, Whittaker MR, Minchin RF, Montero MJ, Toth I. Cellular uptake of densely packed polymer coatings on gold nanoparticles. *ACS Nano*. 2010;4(1):403–13.
- Liu X, Huang N, Li H, Jin Q, Ji J. Surface and size effects on cell interaction of gold nanoparticles with both phagocytic and non-phagocytic cells. *Langmuir*. 2013;29:9138–48.
- Maiorano G, Sabella S, Sorce B, Brunetti V, Malvindi MA, Pompa PP. Effects of cell culture media on the dynamic formation of protein-nanoparticle complexes and influence on the cellular response. *ACS Nano*. 2010;4(12):7481–91.
- Nativo P, Prior IA, Brust M. Uptake and intracellular fate of surface-modified gold nanoparticles. *ACS Nano*. 2008;2(8):1639–44.
- Navya PN, Daima HK. Rational engineering of physicochemical properties of nanomaterials for biomedical applications with nanotoxicological perspectives. *Nano Convergence*. 2016;3(1):1–14.
- Ng CT, Perumalsamy R, Watt F and Yuan YL. Localizing cellular uptake of nanomaterials in vitro by transmission electron microscopy. *Microscopy: Science, technology and education*. Formatted. 2010; 316-320.
- Oh N, Park J. Endocytosis and exocytosis of nanoparticles in mammalian cells. *Int J Nanomedicine*. 2014a;9(Suppl I):51–63.
- Oh N, Park J. Surface chemistry of Gold nanoparticles mediates their exocytosis in macrophages. *ACS Nano*. 2014b;8(6):6232–41.
- Oh E, Delehanty JB, Medintz IL. Cellular uptake and fate of PEGylated gold nanoparticles is dependent on both cell-penetrating peptides and particle size. *ACS Nano*. 2011;5(8):6434–48.
- Otsuka H, Nagasaki Y, Kataoka K. PEGylated nanoparticles for biological and pharmaceutical applications. *Adv Drug Deliv Rev*. 2003;55:403–19.
- Patra CR, Bhattacharya R, Mukhopadhyay D, Mukherjee P. Fabrication of gold nanoparticles for targeted therapy in pancreatic cancer. *Adv Drug Deliv Rev*. 2010;62:346–61.
- Pissuwan D, Cortie CH, Valenzuela SM, Cortie MB. Functionalized gold nanoparticles for controlling pathogenic bacteria. *Trends Biotechnol*. 2010;28(4):207–13.
- Pissuwan D, Niidome T, Cortie MB. The forthcoming applications of gold nanoparticles in drug and gene delivery systems. *J Control Release*. 2011;149:65–71.
- Rocha A, Zhou Y, Kundu S, Liang H. In vivo observation of gold nanoparticles in the central nervous system of *Blaberus discoidalis*. *J Nanobiotechnol*. 2011;9:5.
- Rosi AL, Giljohann DA, Thaxton CS, Lytton-Jean AKR, Han MS, Mirkin CA. Oligonucleotide-modified gold nanoparticle for intracellular gene regulation. *Science*. 2006;312:1027–30.
- Sabuncu AC, Grubbs J, Qian S, Beskok A. Probing nanoparticle interactions in cell culture media. *Colloids Surf B: Biointerfaces*. 2012;95:96–102.
- Sarah B. Breath test to detect cancer may be possible, say scientists. 2010. <http://www.guardian.co.uk/world/2010/aug/11/breath-test-detect-cancer-scientists>
- Shenoy D, Fu W, Li J, Crasto C, Jones G, DiMarzio C, et al. Surface Functionalization of Gold nanoparticles using hetero-bifunctional poly (ethylene glycol) spacer for intracellular tracking and delivery. *Int J Nanomedicine*. 2006;1:51–7.
- Shukla R, Bansal V, Chaudhary M, Basu A, Bhonde RR, Sastry M. Biocompatibility of gold nanoparticles and their



- endocytotic fate inside the cellular compartment. *Langmur*. 2006;21:10644–54.
- Skebo JE, Grabinski CM, Hussain SM. Assessment of metal nanoparticle agglomeration, uptake, and interaction using high-illuminating system. *Int J Toxicol*. 2007;29:135–41.
- Tiwari PM, Vig K, Dennis VA, Singh SR. Functionalized gold nanoparticles and their biomedical applications. *Nanomaterials*. 2011;1:31–63.
- Turkevich J, Stevenson PC, Hillier J. A study of the nucleation and growth processes in the synthesis of colloidal gold. *Discuss Faraday Soc*. 1951;11:55–75.
- Uboldi C, Bonacchi D, Lorenzi G, Hermanns MI, Pohl C, Baldi G, et al. Gold nanoparticles induce cytotoxicity in the alveolar type-II cell lines A549 and NCIH44I. *Part Fibre Toxicol*. 2009. doi:10.1186/1743-8977-1186-1118.
- Ürcan E, Haertel U, Styllou M, Hickel RB, Harry Scherthan H, Reichl FX. Real-time xCELLigence impedance analysis of the cytotoxicity of dental composite components on human gingival fibroblasts. *Dent Mater*. 2010;26:51–8.
- Vetten MA, Tlotleng N, Rascher DT, Skepu A, Keter FK, Gulumian M. Label free in vitro toxicity and uptake assessment of citrate stabilized gold nanoparticles in three cell lines. *Part Fibre Toxicol*. 2013;10(50):1–15.
- Zhang Z, Jia J, Lai Y, Ma Y, Weng J, Sun L. Conjugating folic acid to gold nanoparticles through glutathione for targeting and detecting cancer cells. *Bioorg Med Chem*. 2010;18:5528–34.
- Zhou H, Li X, Lemoh H, Zhang B, Yan B. Structural confirmation and quantification of individual ligands from the surfaces of multi-functionalized gold nanoparticles. *Analyst*. 2010;135: 1210–3.